Cell

Complete Kinetochore Tracking Reveals Error-Prone Homologous Chromosome Biorientation in Mammalian Oocytes

Tomoya S. Kitajima,[1] Miho Ohsugi,[2,3] and Jan Ellenberg[1,*]
[1]Cell Biology and Biophysics Unit, European Molecular Biology Laboratory (EMBL), Meyerhofstrasse 1, Heidelberg D-69117, Germany
[2]Division of Oncology, Department of Cancer Biology, Institute of Medical Science, The University of Tokyo, Minato-ku, Tokyo 108-8639, Japan
[3]PRESTO, Japan Science and Technology Agency, 4-1-8 Honcho Kawaguchi, Saitama 332-0012, Japan
*Correspondence: jan.ellenberg@embl.de
DOI 10.1016/j.cell.2011.07.031

SUMMARY

Chromosomes must establish stable biorientation prior to anaphase to achieve faithful segregation during cell division. The detailed process by which chromosomes are bioriented and how biorientation is coordinated with spindle assembly and chromosome congression remain unclear. Here, we provide complete 3D kinetochore-tracking datasets throughout cell division by high-resolution imaging of meiosis I in live mouse oocytes. We show that in acentrosomal oocytes, chromosome congression forms an intermediate chromosome configuration, the prometaphase belt, which precedes biorientation. Chromosomes then invade the elongating spindle center to form the metaphase plate and start biorienting. Close to 90% of all chromosomes undergo one or more rounds of error correction of their kinetochore-microtubule attachments before achieving correct biorientation. This process depends on Aurora kinase activity. Our analysis reveals the error-prone nature of homologous chromosome biorientation, providing a possible explanation for the high incidence of aneuploid eggs observed in mammals, including humans.

INTRODUCTION

Proper segregation of homologous chromosomes during the first meiotic division in female oocytes is essential to prevent generation of aneuploid eggs. Fertilization of aneuploid eggs in humans is a leading cause of pregnancy loss and, if survived to term, results in developmental disabilities (Hassold and Hunt, 2001). To segregate homologous chromosomes faithfully, it is essential that all bivalents, the paired homologous chromosomes, achieve biorientation, i.e., that their homologous kinetochores are attached to microtubules from the opposite poles of the meiotic spindle. Although the mechanism of sister chromatid biorientation has been well studied in somatic mitotic cells (Kops et al., 2010; Maiato et al., 2004; Walczak and Heald, 2008), homologous chromosome biorientation in animal oocytes is poorly understood.

Somatic animal cells contain two centrosomes that predefine the poles of the mitotic spindle. One of the most widely used models to explain biorientation is the so-called "search-and-capture" mechanism, in which sister kinetochores become attached to microtubules emanating from the spindle poles. If both kinetochores are attached in an end-on manner from opposite poles (amphitelic), the force balance leads to stable biorientation. If the attachment is incorrect, for example if one kinetochore is attached to two poles (merotelic) or both are attached to the same pole (syntelic), the force balance cannot be achieved. Such erroneous attachments are sensed by Aurora B kinase, which phosphorylates a set of kinetochore substrates to detach the incorrect microtubules. The detached kinetochores activate the spindle assembly checkpoint, giving the cell time for a new round of biorientation (Nezi and Musacchio, 2009). Merotelic and syntelic attachments are regarded as errors that must be corrected because they would cause chromosome missegregation if they persisted until anaphase (Cimini et al., 2003). Although no comprehensive quantitative analysis has been carried out, the available data (Cimini et al., 2003) allow estimation of the number of erroneous attachments during prometaphase in somatic mitotic cells to less than 10%, although this may be an underestimate (Salmon et al., 2005). The classical search-and-capture model explains chromosome congression as a result of the biorientation process because the balance of the pulling forces on the sister kinetochores positions the chromosomes at the spindle equator. Although congression mechanisms that do not require biorientation have been described (Cai et al., 2009; Kapoor et al., 2006; Wignall and Villeneuve, 2009), it remains unknown what fraction of chromosomes normally congress without biorientation in mammalian cells (Foley and Kapoor, 2009).

By contrast, oocytes in humans and all other mammals analyzed so far (and also in *Gallus*, *Xenopus*, *Drosophila*, and *C. elegans*) lack centrosomes (Manandhar et al., 2005), and the search-and-capture mechanism should become insufficient in their large cytoplasm (Wollman et al., 2005). Oocytes must

therefore achieve spindle bipolarization and chromosome biorientation through a different process (Walczak and Heald, 2008). Because mice represent the closest experimentally tractable model to humans, we have focused our analysis on their oocytes. We previously showed that the acentrosomal spindle in mouse oocytes is assembled by self-organization of many microtubule-organizing centers (MTOCs) (Schuh and Ellenberg, 2007). Upon nuclear envelope breakdown (NEBD), over 80 MTOCs scattered in the cytoplasm attract each other and form a cluster in the center of the oocyte that radiates microtubules to the outside, the apolar microtubule ball. This ball then bipolarizes through a several hour tug of war of attractive and repulsive forces between the MTOCs, giving rise to multipolar intermediates and ultimately a barrel-shaped spindle with poorly focused poles. How homologous chromosome biorientation is achieved during this lengthy and complex spindle self-assembly process is not known to date.

In this study, we have addressed this issue, using 3D confocal fluorescence microscopy at high spatial and temporal resolution in live mouse oocytes. We succeeded to track all homologous kinetochores during the approximately 8 hr from NEBD to the onset of chromosome segregation in anaphase. These datasets allowed a systematic quantitative analysis of kinetochore and chromosome dynamics during the first meiotic division. We show that chromosome congression precedes biorientation, forming an intermediate chromosome configuration, the prometaphase belt. Furthermore we show that two-thirds of all biorientation attempts are erroneous, and that 86% of all homologous chromosomes undergo error corrections of their kinetochore-microtubule attachments before they establish stable biorientation. These results show that homologous chromosome biorientation is a highly error-prone process in acentrosomal mammalian oocytes, which may explain the high incidence of segregation errors in meiosis I observed in vivo (Hassold and Hunt, 2001).

RESULTS

Tracking of All Kinetochores during Cell Division

To analyze spatiotemporal dynamics of kinetochores and chromosomes during the first meiotic division of live mouse oocytes, we recorded four-dimensional (4D) datasets of kinetochores and chromosomes labeled with EGFP-CENP-C and Histone 2B (H2B)-mCherry, respectively, expressed after quantitative mRNA microinjection (Jaffe and Terasaki, 2004) (Figure 1A; Movie S1 available online). We used an automated confocal microscope that can focus and track all chromosomes within the oocyte to record 3D stacks of optical sections for 9 hr after induction of maturation (Schuh and Ellenberg, 2007; Rabut and Ellenberg, 2004). Live imaging did not perturb oocyte maturation, as the rate of polar body extrusion and average time from NEBD to polar body extrusion were indistinguishable from normal in vitro culture conditions (83% [n = 12 with imaging] versus 78% [n = 61 w/o imaging], p = 1.0; 8.8 ± 0.6 hr [n = 10] versus 8.6 ± 0.8 hr [n = 7], p = 0.7). In these 4D datasets, we could detect 99.6% of all kinetochores (n = 200 from 5 oocytes) at all time points from NEBD to anaphase onset with high spatial (xy 0.3 μm, z 3.0 μm) and temporal (90 s) resolution. The 4D datasets were processed by an in-house-developed computational pipeline, which detects kinetochore positions and tracks them in 3D after registration of global cellular movements. The resulting kinetochore tracks were interactively validated and rare errors corrected. In this manner we could obtain complete 3D tracking datasets of all kinetochores during the entire process of the first meiotic division (Figures 1B and 1E; Movie S2). We make these datasets available online as a resource for the analysis of kinetochore and chromosome dynamics (http://www.ellenberg.embl.de/apps/KTTracking/).

Kinetochore Movements Define Four Kinetic Phases of Chromosome Biorientation

To gain insight into the processes that govern kinetochore dynamics, we analyzed different parameters for reproducible global changes during the first meiotic division. The average kinetochore speed changed in a canonical and stepwise fashion after NEBD (Figures 1C and 1D; Movie S2), suggesting changes in the interactions of kinetochores and/or chromosome arms with microtubules. Thus we can define five kinetic phases of chromosome dynamics during the first meiotic division: phase 1 (~0–1 hr), in which kinetochores move relatively rapidly (0.19 ± 0.04 μm/min, up to 0.31 μm/min) outwards; phase 2 (~1–2 hr), in which kinetochores move more slowly (0.13 ± 0.03 μm/min, up to 0.25 μm/min) with no obvious radial directionality; phase 3 (~2–4 hr), in which chromosomes exhibit rapid oscillations (0.27 ± 0.11 μm/min, up to 0.59 μm/min) along the spindle axis; phase 4 (from ~4 hr to anaphase onset), in which chromosomes oscillate more slowly (0.19 ± 0.05 μm/min, up to 0.34 μm/min); and finally anaphase, during which chromosomes very rapidly move to the opposite spindle poles (0.80 ± 0.23 μm/min, up to 1.2 μm/min). Anaphase is triggered after completion of biorientation, but how chromosome biorientation is achieved during the preceding four phases is poorly understood in mammalian meiosis, and we therefore decided to analyze them in more detail.

In Phase 1, Kinetochores Individualize to a Spherical Shell

We previously reported that clustered chromosomes are individualized and moved onto the forming microtubule ball ~0–1 hr after NEBD (Schuh and Ellenberg, 2007), which corresponds to phase 1. By analyzing kinetochore tracks during phase 1, we found that not only chromosomes but also kinetochores were individualized from their clusters during the chromosome-sorting process (Figures S1A–S1D), resulting in a spherical shell-like chromosome configuration on the surface of the microtubule ball (see also Figure 4).

In Phase 2, Chromosomes Congress to Form the Prometaphase Belt

To understand how the individualized chromosomes congress to the metaphase plate, we carefully analyzed their spatial distribution in three dimensions over time. At the beginning of phase 2, chromosomes and kinetochores were distributed randomly (Figures 2A and 2B, 0:49) on the surface of the microtubule ball (see also Figure 4B). With the onset of chromosome congression, this distribution became progressively ordered as

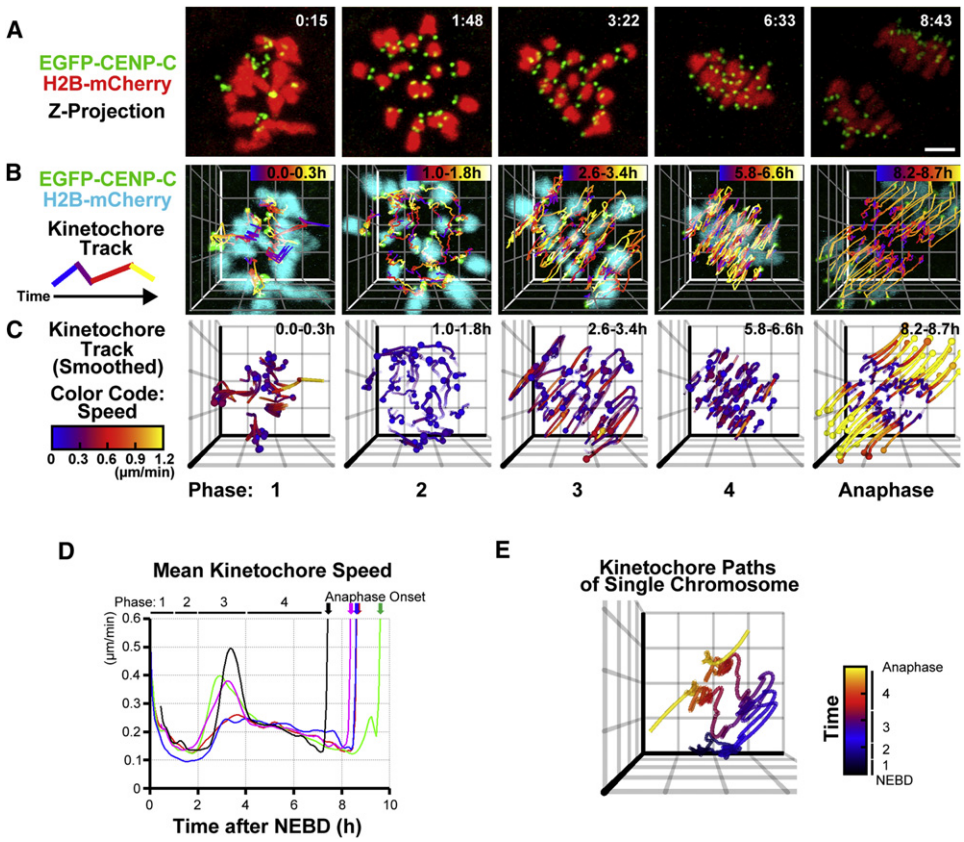

Figure 1. Complete 3D Kinetochore Tracking In Vivo

(A) Time-lapse imaging of the first meiotic division in an oocyte expressing EGFP-CENP-C (kinetochores, green) and H2B-mCherry (chromosomes, red). Maximum intensity z projection images from representative time points for each phase (phase 1, 2, 3, 4, and anaphase) are shown. EGFP-CENP-C signals are processed for peak enhancement and background subtraction. H2B-mCherry signals are processed by a Gaussian filter. Time after NEBD (hr:mm). Scale bar is 5 μm. See also Movie S1.

(B) The images are reconstructed in 3D. The kinetochore (green) and the chromosome (cyan) signals are shown. Kinetochore tracks are indicated by lines and color-coded by time. Time after NEBD (hr). The unit of the grid is 5 μm.

(C) The kinetochore tracks are smoothed and color-coded by the kinetochore speeds as indicated by the color bar. Tracks in earlier time points are shown more transparent.

(D) The mean kinetochore speed of all kinetochores is shown over time. The smoothed curves of 5 oocytes are shown.

(E) Smoothed paths of homologous kinetochores on a single chromosome from NEBD to anaphase onset are shown. The color code represents the time after NEBD as indicated by the color bar. The unit of the grid is 5 μm.

Paths of all chromosomes are available in http://www.ellenberg.embl.de/apps/KTTracking/. See also Figure S1 and Movie S2.

shown by a decrease in aspect ratio of the ellipsoid fitted to all chromosome positions (Figure 2C). At the end of phase 2, all chromosomes had relocated close to the equator of the overall chromosome distribution (Figures 2A–2C, 1:59; Movie S3). Viewing chromosome positions from the top onto the equator revealed that they formed a belt-like arrangement with a chromosome-free region inside of the equator (Figure 2B, top view, 1:59). Thus, chromosome congression results in a belt-like chromosome configuration, which we refer to hereafter as the "prometaphase belt."

To investigate how chromosomes move to the prometaphase belt, we analyzed their tracks during congression. Chromosomes that were located far from the equator at the beginning of phase 2 congressed toward it, whereas chromosomes already located near the equator remained stationary until the end of phase 2 (Figure 2D). The paths of the congressing chromosomes defined arcs around a 7.5 μm radius sphere, consistent with the size of the microtubule ball (see also Figure 4). Collectively, chromosomes therefore congress to form the prometaphase belt by sliding along the surface of the microtubule ball during phase 2 (Figure 3E, "phase 2").

We reasoned that plus-end-directed forces generated by chromokinesins might be responsible for chromosome individualization in phase 1 and/or prometaphase belt formation in phase 2. The chromokinesin Kid is a prime candidate because it has been shown to be required for expulsion of chromosomes on a monopolar spindle in mitotic cells (Levesque and Compton, 2001) and congression in *Xenopus* egg extracts (Antonio et al., 2000; Funabiki and Murray, 2000). We therefore imaged chromosome and kinetochore dynamics in oocytes from Kid knockout

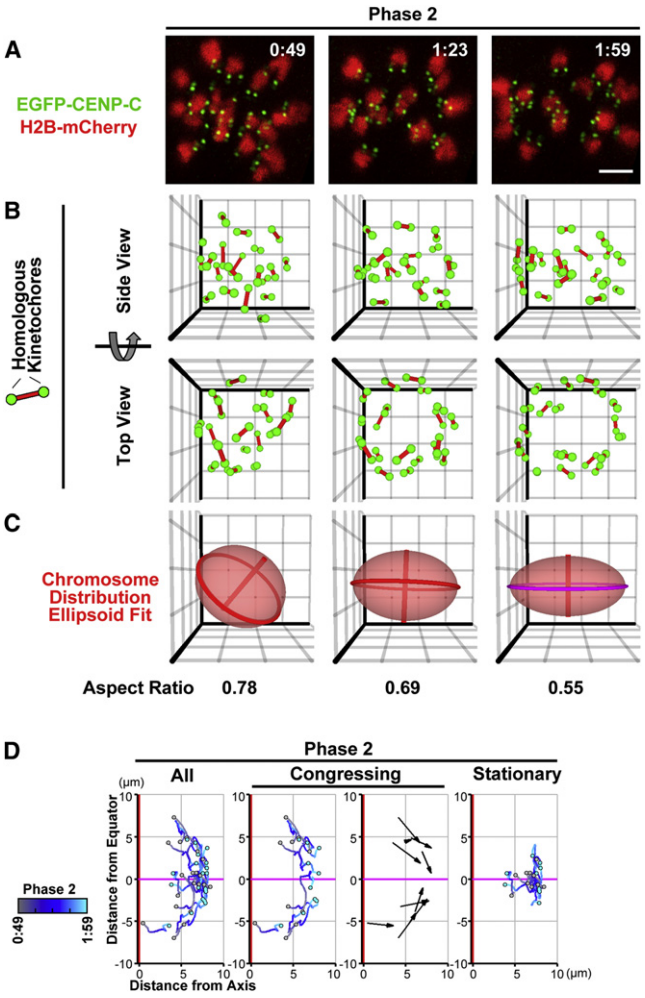

Figure 2. Chromosome Congression Proceeds via the Prometaphase Belt

(A) Images of EGFP-CENP-C (kinetochores, green) and H2B-mCherry (chromosomes, red) in phase 2. The projection view along the chromosome distribution equator (see C) at 1:59 is shown. Time after NEBD (hr:mm). Scale bar is 5 μm.

(B) Kinetochore positions are shown in 3D as green spheres and red bars connecting homologous kinetochores. The views along the chromosome distribution equator at 1:59 (Side View) and perpendicular to the equator (Top View) are shown. The unit of the grid is 5 μm.

(C) Ellipsoids fitted to chromosome distributions (red). The aspect ratio of the ellipsoid (h/w, where h is the length of the ellipsoid shortest axis [red bar], and w is the diameter of the equator [red/magenta circle]) is shown at the bottom. The view along the equator at 1:59 is shown.

(D) Smoothed chromosome tracks from 0:49 to 1:59 (hr:mm) are plotted. The x axis (magenta) and y axis (red) represent the chromosome distribution equator at 1:59 and its shortest axis, respectively, as in (C). The start points of the tracks are shown as gray circles and the end points are shown as cyan circles. The color code represents time as indicated by the color bar. Tracks of all chromosomes (All), the chromosomes congressing to the equator (Congressing), and the chromosomes staying around the equator (Stationary) are shown. Arrows indicate displacement of the "congressing" chromosomes. See also Figure S2 and Movie S3.

mice (Ohsugi et al., 2008) (Figure S2A). Quantitative analysis of these data revealed that neither chromosome individualization nor congression was significantly affected by the absence of Kid (Figures S2B–S2D), demonstrating that Kid is dispensable for these processes in mouse oocytes.

In Phase 3, Chromosomes Invade the Spindle, Transforming the Prometaphase Belt into the Metaphase Plate

Although the prometaphase belt formed during phase 2 represents a congressed chromosome configuration, in that all paired kinetochores are found around one plane, it is not yet the final arrangement in which chromosomes are stably bioriented. Therefore, we next addressed how the prometaphase belt with its chromosome-free interior transforms into the metaphase plate. During phase 3, chromosomes moved from the belt toward the center of the plane (Figures 3A–3D; Movie S3). This centripetal movement resulted in an even distribution of the chromosomes across the equatorial plane by the end of phase 3 (Figure S3A), thereby defining the metaphase plate. Thus, the metaphase plate is formed by chromosomes invading the spindle from the peripheral prometaphase belt (Figure 3E, "phase 3"). Both the change in direction and the significant increase in speed of the invading chromosomes compared to phase 2 (average speed of congressing chromosomes = 0.13 ± 0.02 [n = 10]; average speed of invading chromosomes = 0.17 ± 0.04 [n = 6]; p = 0.01) indicated a different mechanism of this motion. Furthermore, the inward movements were concomitant with the onset of kinetochore oscillations perpendicular to the equator (Figure 3D), suggesting that kinetochore-microtubule attachments are dynamic during the invasion of chromosomes.

Chromosome Congression Precedes Bivalent Stretching

Next, we wanted to determine when bivalents are stretched by directional microtubule forces. By measuring interkinetochore distances, we found that most bivalents were not stretched in phase 2, although they had already congressed, forming the prometaphase belt (Figures 4A and 4D and Movie S4, from −130 to −70 min). During the invasion in phase 3, however, the fraction of stretched bivalents increased progressively, reaching 89% ± 9% (Figures 4A and 4D and Movie S4, from −70 to 50 min). Thus, the majority of bivalents became stretched only after the formation of the prometaphase belt, as indicated by the significantly different half-time of chromosome congression and fraction of stretched bivalents (p = 0.0001, Figure 4E).

Spindle Elongation Promotes Chromosome Biorientation

To examine the relationship of spindle elongation with chromosome biorientation, we imaged kinetochores and microtubules by 3mCherry-CENP-C and EGFP-MAP4, respectively (Figure 4B). During phase 3 the spindle elongated, increasing its aspect ratio almost exactly concomitantly with the increase of stretched bivalents (Figures 4C and 4D, from −70 to 50 min), indicated by indistinguishable half-times of the increases

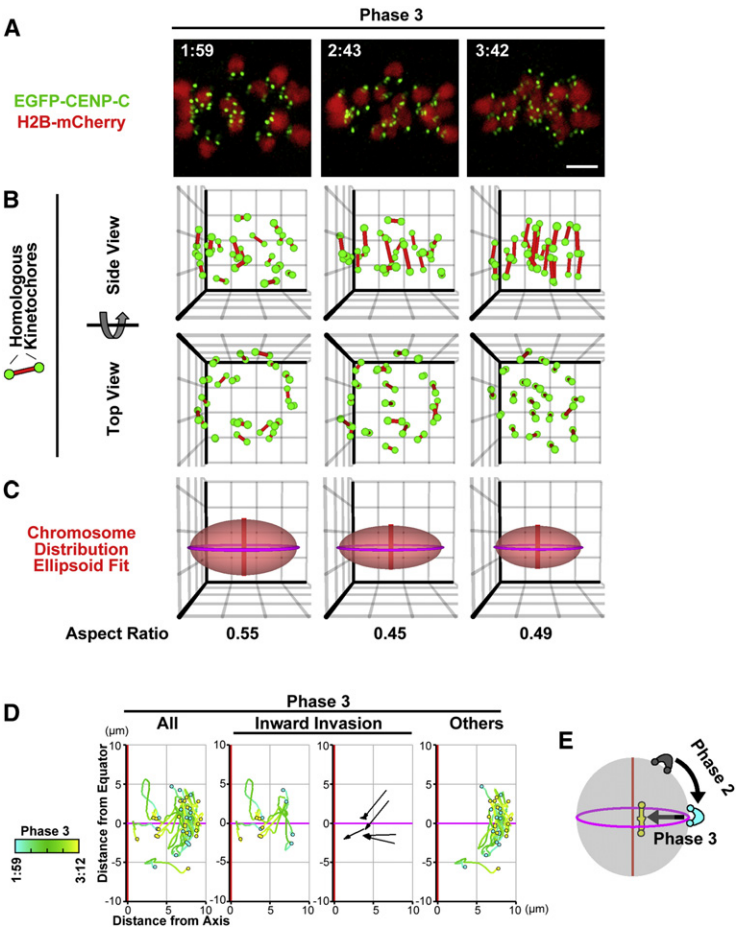

Figure 3. Chromosomes Invade the Spindle to Form the Metaphase Plate

(A) Images of EGFP-CENP-C (kinetochores, green) and H2B-mCherry (chromosomes, red) in phase 3. Time after NEBD (hr:mm). The projection view along the chromosome distribution equator is shown. The scale bar is 5 μm.

(B) Kinetochore positions are shown in 3D as green spheres and red bars connecting homologous kinetochores. The views along the chromosome distribution equator (Side View) and perpendicular to the equator (Top View) are shown. The unit of the grid is 5 μm.

(C) Ellipsoids fitted to chromosome distribution (red). The view along the equator (magenta) is shown. The aspect ratio of the ellipsoid is shown at the bottom.

(D) Smoothed chromosome tracks from 1:59 to 3:12 (hr:mm) are plotted. The x axis (magenta) and y axis (red) represent the chromosome distribution equator and its shortest axis, respectively, as in (C). The start points of the tracks are shown as cyan circles and the end points are shown as yellow circles. The color code represents time as indicated by the color bar. Tracks of all chromosomes (All), the chromosomes moving inward (Inward Invasion), and the other chromosomes (Others) are shown. Arrows indicate displacement of the "inward invasion" chromosomes.

(E) A model for chromosome movement in phases 2 and 3. Chromosomes congress to the equator (magenta circle) sliding along the surface of the microtubule ball and form the prometaphase belt in phase 2 (from gray to cyan). The chromosomes invade the spindle inwards to form the metaphase plate in phase 3 (from cyan to yellow).

See also Figure S3 and Movie S3.

(p = 1.0, Figure 4E). This precise kinetic correlation suggests that spindle elongation contributes to chromosome biorientation.

To understand how homologous chromosomes achieve biorientation, we analyzed dynamics of bivalent stretching and alignment by measuring changes in interkinetochore distances and chromosome angles with the spindle axis, respectively. Average bivalent stretching (Figure 5B) and alignment (Figure 5E) increased progressively with linear kinetics during phase 3 (from −70 to 50 min), confirming that the majority of chromosomes becomes bioriented during spindle elongation (compare Figure 4D).

To analyze the kinetics of individual chromosome biorientation attempts (Figure 5A), we counted the number of significant bivalent stretching events (see Experimental Procedures and Figure S4A) over time. Biorientation attempts occurred most frequently in the first half of phase 3 (Figure 5D, from −50 to 0 min), when the spindle starts to elongate (compare Figure 4D), and oriented the chromosomes parallel to the spindle axis (Figure 5G). By contrast, biorientation attempts that occurred prior to spindle elongation in phase 2 (compare Figure 4D) failed to orient chromosomes along the spindle axis (Figures 5D and 5G, from −150 to −50 min). These results indicate that spindle elongation promotes biorientation and enhances its fidelity.

Loss of Kinetochore Attachment Is the Rule for Chromosome Biorientation in Oocyte Meiosis

The complete kinetochore-tracking datasets allowed us to investigate biorientation systematically for each individual chromosome (Figure 5A; Movie S5 and Movie S6). Analyzing bivalent stretching and alignment at the single-chromosome level revealed that only very few chromosomes achieved biorientation at the first attempt, and the kinetic path taken was very different between individual chromosomes (Figure 5A). The "Red" chromosome, for example, started biorientation and alignment early and gradually as revealed by its slow stretching and early alignment (Figures 5A, 5C, and 5F, from −127 to −28 min, red brackets), eventually leading to stable biorientation in a continuous process over ~1.5 hr. By contrast, the "Black" chromosome started biorientation only very late (−5 min), stretching abruptly and snapping into a parallel position with the spindle axis (Figures 5A, 5C, and 5F, 4 min, white and black arrowheads), leading to biorientation within less than 20 min.

We found that most chromosomes underwent multiple biorientation attempts, indicated by repetitive bivalent stretching/relaxation (Figures 5A and 5C; and Movie S6) and reorientation along the spindle axis (Figure 5F). For example, the "Blue" chromosome showed three biorientation attempts. The first occurred at −45 min, but the bioriented state was lost at 4 min. The second biorientation attempt occurred at 15 min, which however halted transiently at 22 min, and was followed by the third attempt at 35 min (Figures 5A, 5C, and 5F, blue arrowheads), leading to stable biorientation. Overall, 86% of all chromosomes underwent two or more biorientation attempts with a maximum of six

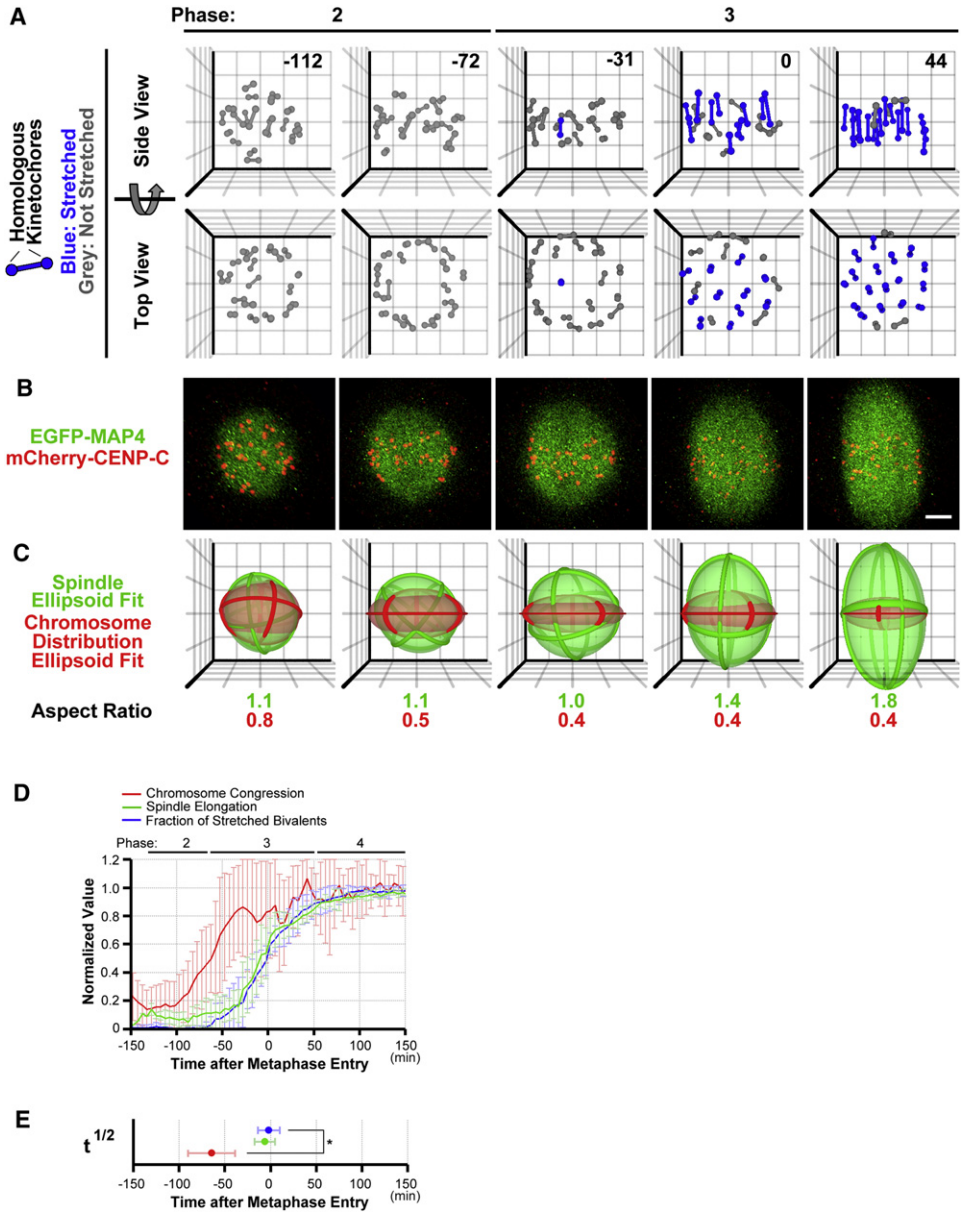

Figure 4. Chromosome Congression Precedes Bivalent Stretching and Spindle Elongation

(A) Kinetochore positions in phases 2 and 3 are shown in 3D as spheres and bars connecting homologous kinetochores. Stretched bivalents (>70% normalized interkinetochore distance) are colored by blue and nonstretched bivalents are colored by gray. The views along the chromosome distribution equator (Side View) and perpendicular to the equator (Top View) are shown. At −112 min, the same view point as that of −72 min is used. The unit of the grid is 5 μm. Time after metaphase entry (min). Phase 2 corresponds to −130 to −70 min. Phase 3 corresponds to −70 to 50 min.

(B) Images of EGFP-MAP4 (microtubule lattices, green) and 3mCherry-CENP-C (kinetochores, red). 3mCherry-CENP-C signals are processed for peak enhancement and background subtraction. The projection view along the chromosome distribution equator is shown. Scale bar is 5 μm.

(C) Ellipsoids fitted to spindle microtubules (green) and chromosome distribution (red). The view along the chromosome distribution equator is shown. The aspect ratios of the ellipsoids are shown at the bottom.

(D) To indicate the extent of chromosome congression (red, n = 9), the aspect ratio of chromosome distribution subtracted from 1 (1 − h/w) is normalized using the minimum value and the mean value over the time points from 100 to 150 min and plotted. To indicate spindle elongation (green, n = 4), the aspect ratio of the spindle is plotted. The values of spindle elongation and fraction of stretched bivalents (blue, n = 9) are normalized using the minimum and the maximum values over all time points. Averages and standard deviations are shown.

(E) The time of the half-maximal value from (D) is plotted. The value of chromosome congression (red) is obtained by fitting a line between the minimum to the last local maximum before metaphase entry. The values of spindle elongation (green) and bivalent stretching (blue) are obtained by fitting sigmoidal curves through all time points. Averages and standard deviations are shown. *p = 0.0001.

See also Movie S4.

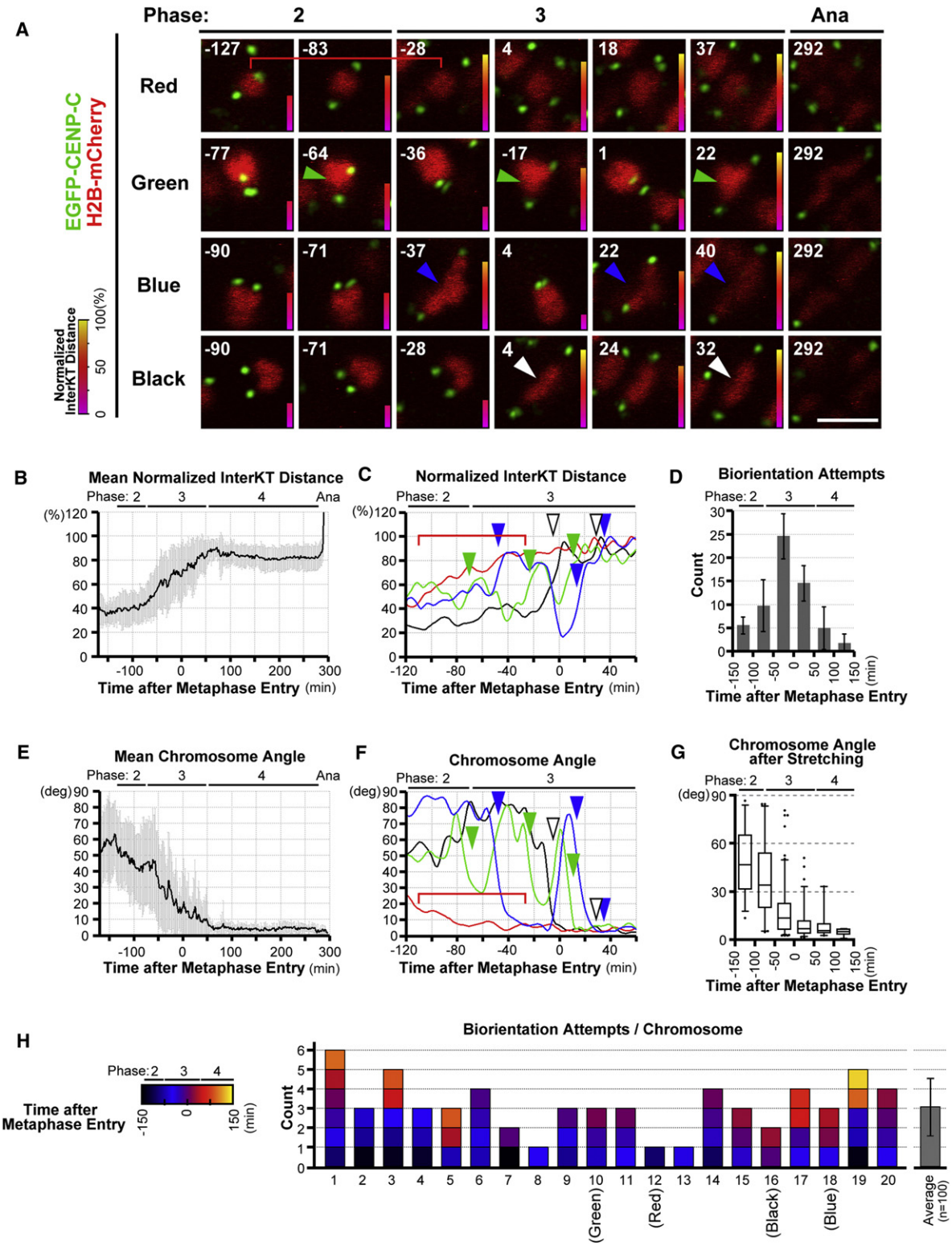

Figure 5. Meiotic Chromosome Biorientation Is Very Error Prone

(A) Images of four single chromosomes in an oocyte expressing EGFP-CENP-C (kinetochores, green) and H2B-mCherry (chromosomes, red). The color bars indicate normalized interkinetochore distances as shown on the left. The text labels denoting colors on the left correspond to the colors used for the plots in (C) and (F). The arrowheads indicate the biorientation attempts (>20% consecutive increase of normalized interkinetochore distance, see also Figure S4A and

and an average of 3.1 ± 1.5 biorientation events per chromosome (Figure 5H, n = 200 from 5 oocytes). Sixty-seven percent of bivalent stretching events collapsed or stalled and were thus not able to establish stable chromosome biorientation. This is most likely due to frequent improper kinetochore-microtubule attachments that would require to be dissolved to be corrected (Nezi and Musacchio, 2009). Indeed, we found that some chromosomes rotated between biorientation events, reverting their orientation between spindle poles (Figure S4C), demonstrating that kinetochore-microtubule attachments were lost and reformed. The dynamic nature of kinetochore-microtubule attachments was additionally indicated by the fact that the amplitude of chromosome oscillations along the spindle axis was maximal in phase 3 (Figures S4D–S4F). Together our results demonstrate that chromosome biorientation is unexpectedly error prone in meiosis I. Most chromosomes underwent multiple kinetochore-microtubule attachments that presumably had to be actively corrected before reaching stable biorientation.

Kinetochore-Microtubule Attachments Are Predominantly Incorrect at Prometaphase

The frequently observed collapse or stalling of bivalent stretching suggested that kinetochore-microtubule attachments are erroneous. Observation of single kinetochore fibers was not possible in live oocytes due to the very high density of non-kinetochore microtubules in the meiotic spindle. To directly investigate kinetochore-microtubule attachments, we therefore immunostained kinetochores and microtubules after destabilizing dynamic non-kinetochore microtubules with calcium in a fixed cell time course (Figure S5G). This allowed us to systematically analyze the nature of the kinetochore-microtubule attachment throughout meiosis (Figures 6A and 6B; and Figure S5H).

Up to 2 hr after NEBD (corresponding to phases 1 and 2), most kinetochores were not attached to microtubule bundles but were contacted by very short microtubules from multiple directions, and we therefore categorized their attachment status as "undefined" (Figures 6A and 6B, 1–2 hr). Starting at 2 hr after NEBD, we found three types of attachments formed by bundled kinetochore microtubules: lateral attachment (microtubules attach to one kinetochore on their sides), merotelic attachment (microtubules from opposite poles attach to one kinetochore on their ends), and amphitelic attachment (microtubules from one pole attach to one kinetochore on their ends) (Figures 6B and 6C and Figure S5H, 2–8 hr). From 2 to 4 hr after NEBD (corresponding to phase 3), merotelic and lateral attachments progressively became more frequent, reaching a maximum 46% ± 15%, whereas amphitelic attachments remained rare (17% ± 8%) (Figure 6C). These merotelic and/or lateral attachments indeed exerted an imbalanced force on the kinetochore as shown by intrakinetochore stretching along the microtubule bundles (Figure S5I). These results indicate that the majority of initial kinetochore attachments to microtubule bundles are not suitable for stable biorientation and are therefore corrected. Indeed amphitelic attachments became more frequent from 4 to 8 hr after NEBD (corresponding to late phase 3 and early phase 4), reaching a maximum of 87% ± 8% (Figures 6A–6C and Figure S5H). These quantitative kinetics of kinetochore attachments derived from fixed cell timecourses are entirely consistent with the frequent collapse or stalling of stretched bivalents observed during phase 3 in our live-cell kinetochore tracking (Figure 6D). If aligned to the same temporal reference of NEBD (Figures S5A–S5F), failed biorientation attempts observed in live cells peak at the time of transition between merotelic and amphitelic attachments in fixed cells (Figures 6C and 6D). It is worth noting that merotelic attachments could be found on apparently well-bioriented chromosomes (Figure 6B, 6 hr, chromosome 1), providing an explanation for the biorientation losses of maximally stretched bivalents observed in live oocytes (compare Figures 5A and 5C, the "Blue" chromosome). These data demonstrate that incorrect kinetochore-microtubule attachments are predominant in prometaphase of meiosis I and are then corrected to amphitelic attachments to establish stable chromosome biorientation required for correct segregation.

Error Correction Requires Aurora B/C Kinase Activity

Our kinetochore-tracking data revealed that most chromosomes undergo multiple biorientation attempts, presumably reflecting error correction of kinetochore-microtubule attachments. In mouse oocytes, it is suggested that Aurora B and potentially also Aurora C are responsible for the error correction (Lane et al., 2010; Sharif et al., 2010; Yang et al., 2010). To examine whether the multiple biorientation attempts depend on the

Experimental Procedures). The bracket indicates the slow biorientation process described in the text. Time after metaphase entry (min). Scale bar is 5 μm. See also Movie S5.

(B) The mean normalized interkinetochore distance of all chromosomes (n = 20) in the oocyte is plotted over time. Error bars represent standard deviations.

(C) Normalized interkinetochore distances for the four chromosomes shown in (A) are plotted over time. The smoothed curves are shown. The arrowheads and the bracket indicate biorientation attempts corresponding to those shown in (A).

(D) Biorientation attempts are counted over time. Averages and standard deviations from 5 oocytes.

(E) The mean chromosome angle with the estimated spindle axis of all chromosomes (n = 20) in the oocyte is plotted over time. Error bars represent standard deviations.

(F) Chromosome angles with the estimated spindle axis for the representative four chromosomes shown in (A) are plotted over time. The smoothed curves are shown. The arrowheads and the bracket correspond to those shown in (A).

(G) Chromosome angles with the estimated spindle axis just after biorientation attempts are plotted in box plots over time. The boxes show the median, 25th, and 75th percentiles, and the bars show the 10th and 90th percentiles (n = 28, 49, 123, 73, 25, 9, from left to right, from 5 oocytes).

(H) The number of biorientation attempts of every chromosome in an oocyte is counted from −150 to 150 min relative to metaphase entry. The color code represents time of the attempt as indicated in the color bar. The bar on the right indicates the average and the standard deviation (n = 100 from 5 oocytes).

Plots of changes in normalized interkinetochore distances and chromosome angles of all chromosomes are available at http://www.ellenberg.embl.de/apps/KTTracking/. See also Figure S4 and Movie S6.

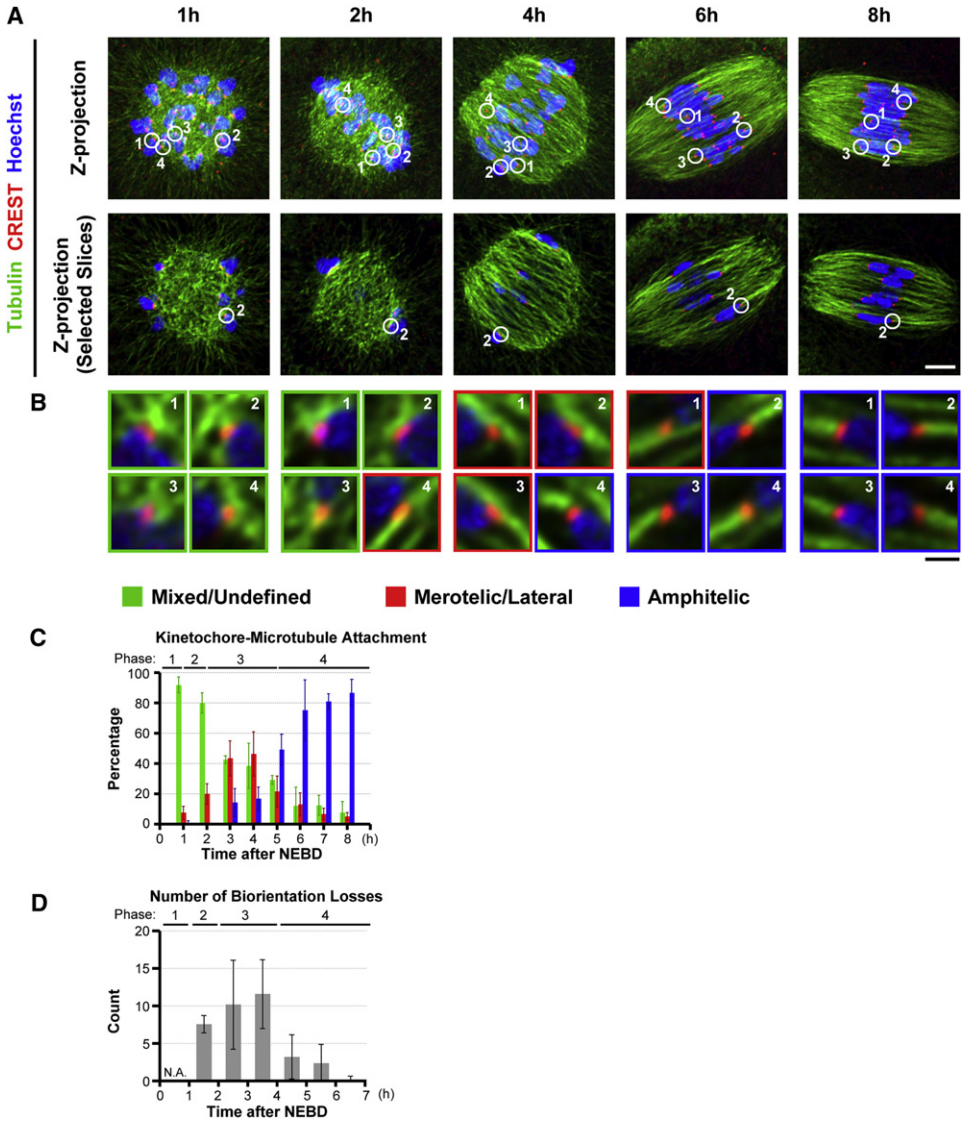

Figure 6. Predominant Improper Kinetochore-Microtubule Attachments in Phase 3

(A) Oocytes were stained with anti-Tubulin (microtubules, green), CREST (kinetochores, red), and Hoechst 33342 (chromosomes, blue) after brief treatment with a 0.1 mM Ca^{2+}-containing buffer (see Extended Experimental Procedures). Maximum intensity z projection images across the whole spindle are shown in the top panel. Z projection images of four selected sections are shown in the bottom panel. Circles and numbers indicate the kinetochores magnified in (B). Time after NEBD (hr). Scale bar is 5 μm.

(B) Magnified views for the kinetochore-microtubule attachments in the oocytes shown in (A). Kinetochore-microtubule attachments are classified into three categories: "Mixed/Undefined" (green), "Merotelic/Lateral" (red), and "Amphitelic" (blue). The images are enwrapped with squares colored according to the categories. Scale bar is 1 μm. The full list of the magnified views for the kinetochore-microtubule attachments are in Figure S5H.

(C) All kinetochores (n = 40) in an oocyte are classified according to their kinetochore-microtubule attachments. The fraction of each category is shown over time, relative to NEBD. Averages and standard deviations from 3 oocytes at each time point are shown. Note that phase 3 is prolonged until 5 hr in this particular experiment, which is evident from quantitative analysis of the chromosome distribution and the spindle (Figures S5A–S5F), presumably because of a temperature control problem during oocyte collection every hour.

(D) Biorientation losses (>20% consecutive decrease of normalized interkinetochore distance) are counted over time from the live imaging data. Averages and standard deviations from 5 oocytes are shown.

activity of Aurora B/C as predicted for error corrections, we treated oocytes with the inhibitor Hesperadin at concentrations that inhibit Aurora B but not Aurora A in somatic cells (Lipp et al., 2007). Hesperadin treatment accelerated the timing of anaphase onset (Figure S6A), consistent with the previously reported Aurora B/C phenotypes in mouse oocytes (Lane et al., 2010; Sharif et al., 2010; Yang et al., 2010). Kinetochore-tracking analysis revealed that the number of biorientation attempts decreased in a dose-dependent manner in Hesperadin-treated oocytes (Figures 7A–7C). Biorientation attempts occurred on

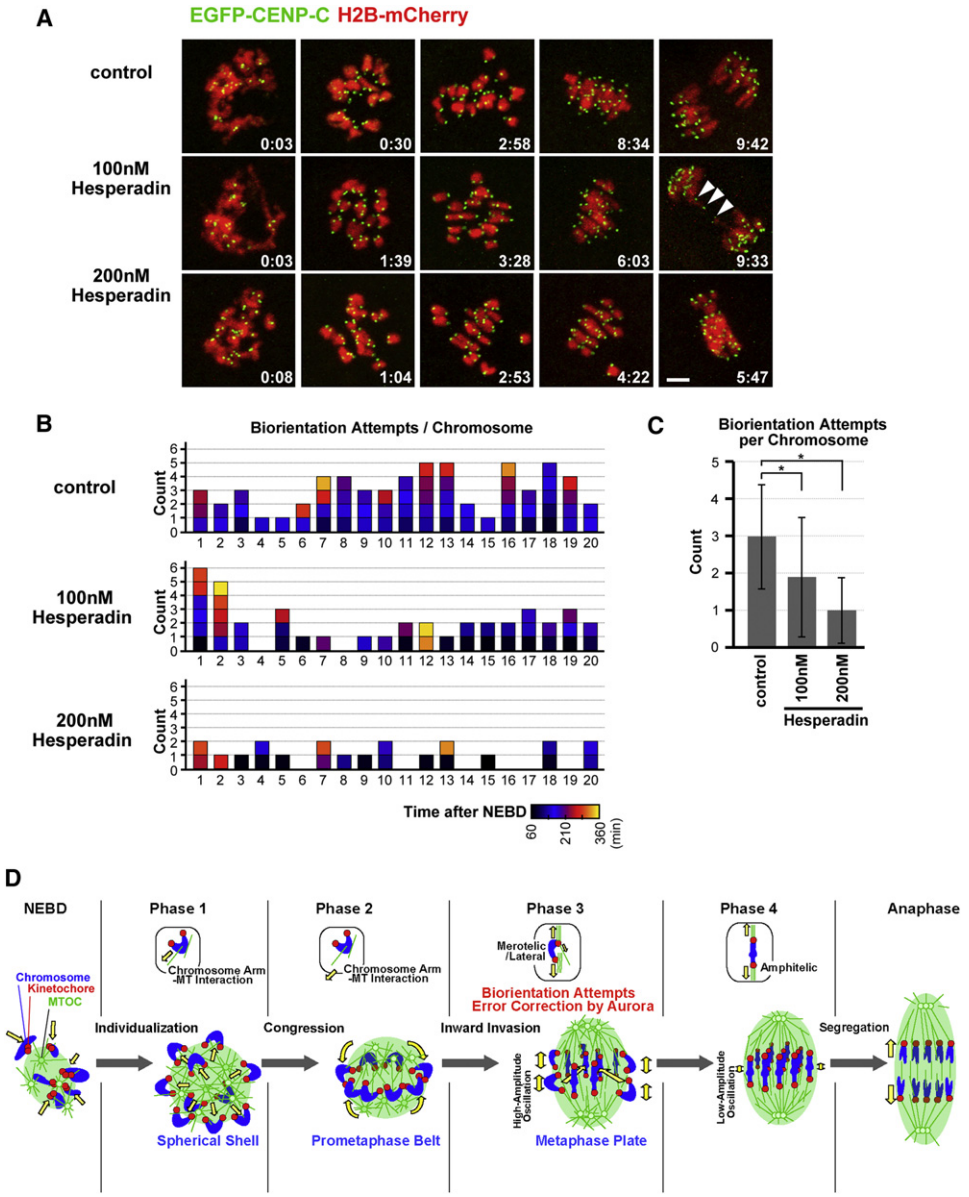

Figure 7. Error Correction Requires Aurora Kinase Activity

(A) Maximum intensity z projection images of EGFP-CENP-C (kinetochores, green) and H2B-mCherry (chromosomes, red) in the presence of DMSO (control) or 100 nM or 200 nM Hesperadin. Time after NEBD (hr:mm). The arrowheads indicate kinetochores on lagging chromosomes. The scale bar is 5 μm.

(B) The number of biorientation attempts of every chromosome in an oocyte is counted from 60 to 360 min after NEBD. The color code represents time of the attempt as indicated in the color bar.

(C) The averages and the standard deviations of the number of biorientation attempts (n = 80, 60, 60 from left to right). *$p < 0.001$.

(D) Model for homologous chromosome biorientation during meiosis I in mouse oocytes. For details, see Discussion.

average only once/chromosome in 200 nM Hesperadin-treated oocytes, suggesting that the first attempt was not corrected in most chromosomes. This effect is consistent with the reported phenotypes of Aurora B knockdown in mitotic cells (Hauf et al., 2003). Furthermore, the same effect was observed after treatment of oocytes with a second, structurally different Aurora B/C inhibitor, ZM447439 (Figure S6B), confirming that Aurora B/C activity is specifically required for multiple biorientation attempts. The effect was not due to the slight shortening of spindle length (86% compared to control oocytes), as oocytes whose spindle lengths were similarly reduced by low-dose Nocodazole treatment showed a normal frequency of biorientation attempts (data not shown). The Hesperadin-treated oocytes exhibited lagging chromosomes (25% at 100 nM [n = 8], 0% in control [n = 10]), and chromosomes failed segregation after short movement toward the spindle poles (100% at 200 nM [n = 5], 0% in control [n = 10]) at anaphase (Figure 7A), indicating that Aurora B/C-dependent error correction is

required for proper chromosome segregation. We conclude that predominant errors in kinetochore-microtubule attachments during prometaphase are converted into correct attachments depending on the activity of Aurora B/C in mouse oocytes.

DISCUSSION

Homologous Chromosome Biorientation Proceeds in Four Phases

Based on changes in dynamic kinetochore parameters, the meiotic process from NEBD to anaphase onset can be divided into four functionally distinct phases (Figure 7D). Before NEBD, chromosomes and kinetochores are clustered, and—after a brief movement caused by NEBD—chromosome-microtubule interactions are initiated. In phase 1, chromosomes move to the surface of the forming microtubule ball, a cluster of MTOCs that continuously polymerize microtubules with their plus ends facing outwards (Schuh and Ellenberg, 2007), distributing as single objects in a spherical shell with individualized kinetochores. In phase 2, chromosomes congress by lateral sliding along the surface of the microtubule ball, forming the prometaphase belt between the future spindle poles. In phase 3, the microtubule ball elongates perpendicular to the prometaphase belt, transforming into the barrel-shaped bipolar spindle. Kinetochores are now subject to stretching forces and attempt biorientation multiple times while oscillating along the spindle axis with high amplitudes. This highly dynamic phase leads to establishment of stable biorientation only after several failed attempts. Concomitantly, stretched chromosomes invade the spindle, transforming the prometaphase belt into the metaphase plate. In phase 4, chromosomes have reached stable biorientation and position on the metaphase plate but continue to show low-amplitude oscillations. Finally, all chromosomes are synchronously segregated toward the opposite poles at anaphase (see also Movie S6).

Chromosome Individualization Is Likely Driven by Chromokinesins

The individualization of chromosomes and their kinetochores in phase 1 is microtubule dependent (Schuh and Ellenberg, 2007), and three arguments make chromokinesins, plus-end-directed motors that bind to chromosome arms, its likely driving force. First, chromosome arms are the main microtubule contacts at this stage (Schuh and Ellenberg, 2007), whereas there are few, if any, kinetochore-microtubule bundles (Figures 6A–6C). Second, chromosomes moved with their arms leading ahead of their kinetochores (Figure S1A; Movie S1 and Movie S2), indicating that the force is transmitted to the arms directly. Third, the chromosome speed was 0.24 μm/min, very similar to the 0.3 μm/min polar ejection movements by a chromokinesin in *Xenopus* egg extracts (Antonio et al., 2000; Funabiki and Murray, 2000).

Formation of the Prometaphase Belt: Redirection of Plus-End-Directed Forces by Bipolarization

During phase 2, chromosomes congress on the surface of the microtubule ball to form the prometaphase belt. Reanalysis of the chromosome configuration in our previous 3D datasets of monastrol-treated oocytes shows that not only bipolarization of the microtubule ball (Schuh and Ellenberg, 2007) but also congression are dependent on kinesin-5, a plus-end-directed motor that slides antiparallel microtubules apart (Kapitein et al., 2005). Although congression occurred before measurable spindle elongation (Figure 4), our immunostaining revealed that stable microtubules indeed start to bipolarize in phase 2, concomitant with congression (Figure 6A and Figure S5D, 2 hr). Our quantitative data furthermore allow us to evaluate three candidate motors for congression. First, congression was completed prior to interkinetochore stretching, ruling out that the pulling force of kinetochore-microtubules from opposite poles (Maiato et al., 2004; Walczak and Heald, 2008; Kops et al., 2010) drives congression. Second, chromosome speed during congression was 0.17 μm/min (max 0.35 μm/min), making it less likely that CENP-E-mediated lateral sliding, known to proceed at 1–2 μm/min (Cai et al., 2009; Kapoor et al., 2006), is responsible. This makes the third candidate, congression driven by chromokinesin-mediated polar ejection forces (Antonio et al., 2000; Funabiki and Murray, 2000), the most likely mechanism. The same forces that individualize chromosomes to the surface of the microtubule ball would thus be redirected by the beginning bipolarization of the spindle and move the chromosomes to the prometaphase belt. The slowing down of the chromosome motion from 0.24 to 0.17 μm/min could be due to an imperfectly bipolarized microtubule ball, which would likely require chromokinesins to switch between microtubules to reach the most distal plus ends on the ball surface. As it has been suggested that chromosome congression depends on a chromokinesin in *C. elegans* oocytes (Wignall and Villeneuve, 2009), the mechanism of congression in acentrosomal oocytes may be conserved among organisms. Furthermore, recent observations of a belt-like structure in prometaphase of somatic cells (Magidson et al., 2011 [this issue of *Cell*]) suggest that the formation of such an intermediate may be a universal mechanism for congression. Kid, a chromokinesin generating a plus-end-directed force in mitosis (Levesque and Compton, 2001) and *Xenopus* egg extracts (Antonio et al., 2000; Funabiki and Murray, 2000), was not essential for chromosome individualization and prometaphase belt formation in mouse oocytes (Figure S2). It will be very interesting to identify the plus-end-directed motor(s) responsible for chromosome individualization and congression in mouse oocytes in future studies.

Kinetochore Fiber-Driven Biorientation Starts in Prometaphase, Transforming the Belt into a Plate

In phase 3, chromosomes start to invade the interior of the prometaphase belt, concomitant with interkinetochore stretching (Figure S3B) and rapid oscillation along the spindle axis (Figure 3D), suggesting that kinetochore-microtubule bundles formed along the spindle axis during phase 3 (Figure 6) are responsible for this motion. The invasion of chromosomes is therefore likely driven by the minimization of the pole-to-pole distances of the pulling microtubules. Kinetochore fibers, amphitelically attached microtubule bundles, could be detected for over 3 hr during phases 3 and 4 (Figure 6), earlier than in

a previous electron microscopy report that could not sample kinetochores systematically (Brunet et al., 1999).

Chromosome Biorientation in Oocytes Is Very Error Prone

Our live- and fixed-cell measurements suggested that kinetochores become initially predominantly attached in an incorrect manner to microtubule bundles (Figure 6), and that consequently 86% of chromosomes undergo two or more rounds of biorientation (Figure 5). This highly error-prone nature of meiotic chromosome biorientation is very interesting in light of the higher incidence of aneuploidies after the first meiotic division in mammalian oocytes, compared to centrosomal somatic mitosis and male meiosis (Hassold and Hunt, 2001).

What could explain this high error rate? Our data suggest that the major reason is the acentrosomal spindle self-assembly process. When kinetochores start to be attached during phase 3, the spindle is only partially bipolarized, with many MTOCs still located far away from the poles (Figure S5D) (Schuh and Ellenberg, 2007), whose microtubules are likely to attach to kinetochores incorrectly (Figure 5). In addition, our kinetochore-tracking data indicate that bivalents in mouse oocytes lack a back-to-back geometrical configuration of homologous kinetochores prior to chromosome biorientation, a mechanism that has been suggested to facilitate efficient homolog biorientation in *Drosophila* and yeasts (Dernburg et al., 1996; Karpen et al., 1996; Kemp et al., 2004; Yokobayashi and Watanabe, 2005). The fact that we used young (8-week-old) mice and did not observe any precocious separation of homologous chromosomes (n = 400 bivalents from 10 oocytes) makes it unlikely that the recently reported age-dependent loss of chromosome cohesion (Hodges et al., 2005; Chiang et al., 2010; Lister et al., 2010) played a role in our experiments. It is furthermore worth noting that we found no correlation between the chiasma-centromere distance and the number of biorientation attempts or time of stable biorientation establishment (Figure S4B and data not shown) and can therefore not corroborate the notion that chiasmata positioned far from the centromere increase the rate of missegregation (Lamb et al., 1997; Hassold et al., 1995; Ross et al., 1996; Koehler et al., 1996; Lacefield and Murray, 2007).

Mouse Oocytes Actively Correct Erroneous Kinetochore Attachments and Exhibit Spindle Checkpoint Activity

For the large majority of chromosomes, erroneous kinetochore-microtubule attachments are dissolved and corrected, as indicated by multiple stalled and/or collapsed biorientation attempts, depending on the Aurora B/C kinase activity (Figure 5 and Figure 7). In mitosis, merotelic attachments are dissolved in an Aurora B-dependent manner, creating unattached kinetochores with an active spindle checkpoint for a new round of attachment (Nezi and Musacchio, 2009). It is likely that this pathway functions also in mouse oocytes, and indeed we found Mad2-EGFP, a spindle checkpoint protein that marks unattached kinetochores (Waters et al., 1998; Chen et al., 1996), on the bivalent kinetochores during phase 3 (Figures S6C and S6D). Consistent with this observation, spindle checkpoint proteins have been shown to be required to prevent errors in chromosome segregation in mouse oocytes (Li et al., 2009; McGuinness et al., 2009; Tsurumi et al., 2004; Wassmann et al., 2003; Homer et al., 2005).

Biorientation during Acentrosomal Spindle Assembly: Stepwise Activation of Chromosome-Microtubule Interactions Coupled to Efficient Error Correction

Taking all our data together, we propose the following mechanism of homologous chromosome biorientation. Initially, chromosomes interact with MTOC microtubules on their arms via chromokinesins to individualize their kinetochores on the surface of the microtubule ball and keep them in reaching distance of microtubules in the large oocyte cytoplasm. The subsequent onset of kinesin-5-dependent bipolarization of the microtubule ball redirects plus-end-directed forces toward its equator, driving congression and creating the prometaphase belt. Until this point, 2 hr after NEBD, kinetochore attachments appear to be suppressed, likely to prevent massively incorrect attachments during the a/multipolar stages of spindle self-assembly. After congression is achieved, kinetochore attachments are allowed but remain highly dynamic to allow multiple rounds of error corrections during the ongoing bipolarization and elongation of the spindle. Finally, kinetochore attachments are stabilized in metaphase and satisfy the spindle checkpoint (as indicated by dissociation of Mad2, Figures S6C and S6D), and anaphase is initiated. In this temporally and spatially well-coordinated manner, homologous chromosome biorientation can be ensured over the course of the long and complex multipolar spindle self-assembly process.

EXPERIMENTAL PROCEDURES

Kinetochore Tracking

In brief, kinetochore positions were detected after signal interpolation in z by the Imaris (Bitplane) spot detection function, followed by manual corrections. To correct global cellular movements, kinetochore positions over time were registered to the centroid of all kinetochores and then tracked using Imaris 3D spot tracking. The tracks were evaluated and the rare errors were corrected manually in Imaris. This left fewer than 0.5% ambiguous kinetochore tracks when two kinetochores of a homologous pair crossed too closely or when kinetochores were clustered at NEBD. See the Extended Experimental Procedures for further detail.

Quantitative Analysis and Visualization

To calculate kinetochore speeds, we fitted cubic smoothing splines to the kinetochore tracks and calculated their derivatives with respect to time to yield the speed (Movie S2). We excluded the values of <5 min after NEBD from the speed analysis of phase 1, when kinetochores moved inwards following the collapse of the nuclear envelope.

Chromosome distribution and the spindle were fitted with ellipsoids, whose equators and diameters were calculated (see Extended Experimental Procedures). When indicated, the images were processed by 3D rotation and maximum intensity projection using ImageJ (http://rsbweb.nih.gov/ij/) to show the projection view along the equator of the chromosome distribution.

To measure homologous chromosome biorientation, we used two parameters, interkinetochore distance and chromosome orientation. The interkinetochore distance, the distance between homologous kinetochores, was normalized to the value of maximal stretching, to account for differences in chiasma positions. Chromosome orientation was measured as the angle between the axis connecting homologous kinetochores and the estimated spindle axis (see Extended Experimental Procedures). When indicated, cubic smoothing splines were fitted to the changes of the normalized interkinetochore distance and the chromosome angle over time. For the calculations described below, we used the smoothed values.

Chromosome biorientation attempts were defined as the events that show >20% consecutive increase of the normalized interkinetochore distance, which were specifically observed from −150 to 150 min after metaphase entry but not for 60 min before anaphase onset (Figure S4A). Stretched bivalents were defined as the chromosomes that reach >70% of their maximal interkinetochore distance. If a stretched bivalent maintained the angle with the estimated spindle axis within <15° until anaphase onset, the chromosome was considered as established orientation along the spindle axis.

We used two different time references during meiosis. One is time after NEBD, which is defined as the time when the diameter of the disassembling nucleolus becomes less than 5 μm. The other is time after metaphase entry, which is defined as the time when half of chromosomes established orientation along the spindle axis.

All calculations were automated by an in-house developed Java (Sun Microsystems) program and R (http://www.r-project.org/). The 2D and the 3D plots were generated by the plotting software Gnuplot (http://www.gnuplot.info/) or Prism (GraphPad) and the ray-tracing software Pov-Ray (http://www.povray.org/), respectively, controlled by scripts generated from the Java program.

SUPPLEMENTAL INFORMATION

Supplemental Information includes Extended Experimental Procedures, six figures, and six movies and can be found with this article online at doi:10.1016/j.cell.2011.07.031.

ACKNOWLEDGMENTS

We thank Alexey Khodjakov for communicating unpublished results; Yoshinori Watanabe for providing mouse CENP-C cDNA and discussion; Andrea Musacchio for providing human Mad2 cDNA; Melina Schuh, Kota Miura, Sebastien Huet, Annelie Wünsche, Thomas Walter, and the members of the Ellenberg lab for advice and discussion; the members of EMBL Laboratory Animal Resources, especially Klaus Schmitt, Silke Brohn, and Angela Burro, for excellent support. This work was supported by HFSP Long-Term Fellowships and JSPS Postdoctoral Fellowships for Research Abroad (to T.S.K.), Grants-in-aid from the Japan Science and Technology Agency and the Ministry of Education, Culture, Sports, Science and Technology, Japan (to M.O.), and the German Research Council as well as the European Commission (DFG EL-246/4-1 within the SPP1384; FP7/2007-2013-241548 within the MitoSys consortium, both to J.E.).

Received: September 9, 2010
Revised: May 17, 2011
Accepted: July 25, 2011
Published: August 18, 2011

REFERENCES

Antonio, C., Ferby, I., Wilhelm, H., Jones, M., Karsenti, E., Nebreda, A.R., and Vernos, I. (2000). Xkid, a chromokinesin required for chromosome alignment on the metaphase plate. Cell *102*, 425–435.

Brunet, S., Maria, A.S., Guillaud, P., Dujardin, D., Kubiak, J.Z., and Maro, B. (1999). Kinetochore fibers are not involved in the formation of the first meiotic spindle in mouse oocytes, but control the exit from the first meiotic M phase. J. Cell Biol. *146*, 1–12.

Cai, S., O'Connell, C.B., Khodjakov, A., and Walczak, C.E. (2009). Chromosome congression in the absence of kinetochore fibres. Nat. Cell Biol. *11*, 832–838.

Chen, R.H., Waters, J.C., Salmon, E.D., and Murray, A.W. (1996). Association of spindle assembly checkpoint component XMAD2 with unattached kinetochores. Science *274*, 242–246.

Chiang, T., Duncan, F.E., Schindler, K., Schultz, R.M., and Lampson, M.A. (2010). Evidence that weakened centromere cohesion is a leading cause of age-related aneuploidy in oocytes. Curr. Biol. *20*, 1522–1528.

Cimini, D., Moree, B., Canman, J.C., and Salmon, E.D. (2003). Merotelic kinetochore orientation occurs frequently during early mitosis in mammalian tissue cells and error correction is achieved by two different mechanisms. J. Cell Sci. *116*, 4213–4225.

Dernburg, A.F., Sedat, J.W., and Hawley, R.S. (1996). Direct evidence of a role for heterochromatin in meiotic chromosome segregation. Cell *86*, 135–146.

Funabiki, H., and Murray, A.W. (2000). The Xenopus chromokinesin Xkid is essential for metaphase chromosome alignment and must be degraded to allow anaphase chromosome movement. Cell *102*, 411–424.

Foley, E.A., and Kapoor, T.M. (2009). Chromosome congression: on the bi-orient express. Nat. Cell Biol. *11*, 787–789.

Hauf, S., Cole, R.W., LaTerra, S., Zimmer, C., Schnapp, G., Walter, R., Heckel, A., van Meel, J., Rieder, C.L., and Peters, J.M. (2003). The small molecule Hesperadin reveals a role for Aurora B in correcting kinetochore-microtubule attachment and in maintaining the spindle assembly checkpoint. J. Cell Biol. *161*, 281–294.

Hassold, T., and Hunt, P. (2001). To err (meiotically) is human: the genesis of human aneuploidy. Nat. Rev. Genet. *2*, 280–291.

Hassold, T., Merrill, M., Adkins, K., Freeman, S., and Sherman, S. (1995). Recombination and maternal age-dependent nondisjunction: molecular studies of trisomy 16. Am. J. Hum. Genet. *57*, 867–874.

Hodges, C.A., Revenkova, E., Jessberger, R., Hassold, T.J., and Hunt, P.A. (2005). SMC1beta-deficient female mice provide evidence that cohesins are a missing link in age-related nondisjunction. Nat. Genet. *37*, 1351–1355.

Homer, H.A., McDougall, A., Levasseur, M., Yallop, K., Murdoch, A.P., and Herbert, M. (2005). Mad2 prevents aneuploidy and premature proteolysis of cyclin B and securin during meiosis I in mouse oocytes. Genes Dev. *19*, 202–207.

Jaffe, L.A., and Terasaki, M. (2004). Quantitative microinjection of oocytes, eggs, and embryos. Methods Cell Biol. *74*, 219–242.

Kapitein, L.C., Peterman, E.J.G., Kwok, B.H., Kim, J.H., Kapoor, T.M., and Schmidt, C.F. (2005). The bipolar mitotic kinesin Eg5 moves on both microtubules that it crosslinks. Nature *435*, 114–118.

Kapoor, T.M., Lampson, M.A., Hergert, P., Cameron, L., Cimini, D., Salmon, E.D., McEwen, B.F., and Khodjakov, A. (2006). Chromosomes can congress to the metaphase plate before biorientation. Science *311*, 388–391.

Karpen, G.H., Le, M.H., and Le, H. (1996). Centric heterochromatin and the efficiency of achiasmate disjunction in Drosophila female meiosis. Science *273*, 118–122.

Kemp, B., Boumil, R.M., Stewart, M.N., and Dawson, D.S. (2004). A role for centromere pairing in meiotic chromosome segregation. Genes Dev. *18*, 1946–1951.

Koehler, K.E., Boulton, C.L., Collins, H.E., French, R.L., Herman, K.C., Lacefield, S.M., Madden, L.D., Schuetz, C.D., and Hawley, R.S. (1996). Spontaneous X chromosome MI and MII nondisjunction events in Drosophila melanogaster oocytes have different recombinational histories. Nat. Genet. *14*, 406–414.

Kops, G.J.P.L., Saurin, A.T., and Meraldi, P. (2010). Finding the middle ground: how kinetochores power chromosome congression. Cell. Mol. Life Sci. *67*, 2145–2161.

Lacefield, S., and Murray, A.W. (2007). The spindle checkpoint rescues the meiotic segregation of chromosomes whose crossovers are far from the centromere. Nat. Genet. *39*, 1273–1277.

Lamb, N.E., Feingold, E., Savage, A., Avramopoulos, D., Freeman, S., Gu, Y., Hallberg, A., Hersey, J., Karadima, G., Pettay, D., et al. (1997). Characterization of susceptible chiasma configurations that increase the risk for maternal nondisjunction of chromosome 21. Hum. Mol. Genet. *6*, 1391–1399.

Lane, S.I.R., Chang, H.-Y., Jennings, P.C., and Jones, K.T. (2010). The Aurora kinase inhibitor ZM447439 accelerates first meiosis in mouse oocytes by overriding the spindle assembly checkpoint. Reproduction *140*, 521–530.

Levesque, A.A., and Compton, D.A. (2001). The chromokinesin Kid is necessary for chromosome arm orientation and oscillation, but not congression, on mitotic spindles. J. Cell Biol. *154*, 1135–1146.

Li, M., Li, S., Yuan, J., Wang, Z.B., Sun, S.C., Schatten, H., and Sun, Q.Y. (2009). Bub3 is a spindle assembly checkpoint protein regulating chromosome segregation during mouse oocyte meiosis. PLoS ONE *4*, e7701.

Lipp, J.J., Hirota, T., Poser, I., and Peters, J.-M. (2007). Aurora B controls the association of condensin I but not condensin II with mitotic chromosomes. J. Cell Sci. *120*, 1245–1255.

Lister, L.M., Kouznetsova, A., Hyslop, L.A., Kalleas, D., Pace, S.L., Barel, J.C., Nathan, A., Floros, V., Adelfalk, C., Watanabe, Y., et al. (2010). Age-related meiotic segregation errors in mammalian oocytes are preceded by depletion of cohesin and Sgo2. Curr. Biol. *20*, 1511–1521.

Magidson, V., O'Connell, C.B., Lončarek, J., Paul, R., Mogilner, A., and Khodjakov, A. (2011). The spatial arrangement of chromosomes during prometaphase facilitates spindle assembly. Cell *146*, this issue, 555–567.

Maiato, H., DeLuca, J., Salmon, E.D., and Earnshaw, W.C. (2004). The dynamic kinetochore-microtubule interface. J. Cell Sci. *117*, 5461–5477.

Manandhar, G., Schatten, H., and Sutovsky, P. (2005). Centrosome reduction during gametogenesis and its significance. Biol. Reprod. *72*, 2–13.

McGuinness, B.E., Anger, M., Kouznetsova, A., Gil-Bernabé, A.M., Helmhart, W., Kudo, N.R., Wuensche, A., Taylor, S., Hoog, C., Novak, B., and Nasmyth, K. (2009). Regulation of APC/C activity in oocytes by a Bub1-dependent spindle assembly checkpoint. Curr. Biol. *19*, 369–380.

Nezi, L., and Musacchio, A. (2009). Sister chromatid tension and the spindle assembly checkpoint. Curr. Opin. Cell Biol. *21*, 785–795.

Ohsugi, M., Adachi, K., Horai, R., Kakuta, S., Sudo, K., Kotaki, H., Tokai-Nishizumi, N., Sagara, H., Iwakura, Y., and Yamamoto, T. (2008). Kid-mediated chromosome compaction ensures proper nuclear envelope formation. Cell *132*, 771–782.

Rabut, G., and Ellenberg, J. (2004). Automatic real-time three-dimensional cell tracking by fluorescence microscopy. J. Microsc. *216*, 131–137.

Ross, L.O., Maxfield, R., and Dawson, D. (1996). Exchanges are not equally able to enhance meiotic chromosome segregation in yeast. Proc. Natl. Acad. Sci. USA *93*, 4979–4983.

Salmon, E.D., Cimini, D., Cameron, L.A., and DeLuca, J.G. (2005). Merotelic kinetochores in mammalian tissue cells. Philos. Trans. R. Soc. Lond. B Biol. Sci. *360*, 553–568.

Schuh, M., and Ellenberg, J. (2007). Self-organization of MTOCs replaces centrosome function during acentrosomal spindle assembly in live mouse oocytes. Cell *130*, 484–498.

Sharif, B., Na, J., Lykke-Hartmann, K., McLaughlin, S.H., Laue, E., Glover, D.M., and Zernicka-Goetz, M. (2010). The chromosome passenger complex is required for fidelity of chromosome transmission and cytokinesis in meiosis of mouse oocytes. J. Cell Sci. *123*, 4292–4300.

Tsurumi, C., Hoffmann, S., Geley, S., Graeser, R., and Polanski, Z. (2004). The spindle assembly checkpoint is not essential for CSF arrest of mouse oocytes. J. Cell Biol. *167*, 1037–1050.

Wignall, S.M., and Villeneuve, A.M. (2009). Lateral microtubule bundles promote chromosome alignment during acentrosomal oocyte meiosis. Nat. Cell Biol. *11*, 839–844.

Walczak, C.E., and Heald, R. (2008). Mechanisms of mitotic spindle assembly and function. Int. Rev. Cytol. *265*, 111–158.

Wassmann, K., Niault, T., and Maro, B. (2003). Metaphase I arrest upon activation of the Mad2-dependent spindle checkpoint in mouse oocytes. Curr. Biol. *13*, 1596–1608.

Waters, J.C., Chen, R.H., Murray, A.W., and Salmon, E.D. (1998). Localization of Mad2 to kinetochores depends on microtubule attachment, not tension. J. Cell Biol. *141*, 1181–1191.

Wollman, R., Cytrynbaum, E.N., Jones, J.T., Meyer, T., Scholey, J.M., and Mogilner, A. (2005). Efficient chromosome capture requires a bias in the 'search-and-capture' process during mitotic-spindle assembly. Curr. Biol. *15*, 828–832.

Yang, K.-T., Li, S.-K., Chang, C.-C., Tang, C.-J.C., Lin, Y.-N., Lee, S.-C., and Tang, T.K. (2010). Aurora-C kinase deficiency causes cytokinesis failure in meiosis I and production of large polyploid oocytes in mice. Mol. Biol. Cell *21*, 2371–2383.

Yokobayashi, S., and Watanabe, Y. (2005). The kinetochore protein Moa1 enables cohesion-mediated monopolar attachment at meiosis I. Cell *123*, 803–817.